

# Probing the Galaxy

## I. The galactic structure towards the galactic pole

Y.K. Ng<sup>1,2,5(present address)</sup>, G. Bertelli<sup>3,4</sup>, C. Chiosi<sup>3</sup>, and A. Bressan<sup>5</sup>

<sup>1</sup> Leiden Observatory, P.O. Box 9513, 2300 RA Leiden, the Netherlands

<sup>2</sup> IAP, CNRS, 98 bis Boulevard Arago, F-75014 Paris, France

<sup>3</sup> Department of Astronomy, Vicolo dell'Osservatorio 5, I-35122 Padua, Italy

<sup>4</sup> National Council of Research, CNR – GNA, Rome, Italy

<sup>5</sup> Padova Astronomical Observatory, Vicolo dell'Osservatorio 5, I-35122 Padua, Italy

E-mail: (bertelli, bressan, chiosi, yuen)@astrpd.pd.astro.it

Received 9 November 1995 / Accepted 20 January 1997

**Abstract.** Observations of (B–V) colour distributions towards the galactic poles are compared with those obtained from synthetic colour-magnitude diagrams to determine the major constituents in the disc and spheroid. The disc is described with four stellar sub-populations: the *young*, *intermediate*, *old* and *thick disc* populations, which have respectively scale heights of 100 pc, 250 pc, 0.5 kpc, and 1.0 kpc. The spheroid is described with stellar contributions from the *bulge* and *halo*. The bulge is not well constrained with the data analyzed in this study. A non-flattened power-law describes the observed distributions at fainter magnitudes better than a deprojected  $R^{1/4}$ -law. Details about the age, metallicity, and normalizations are listed in Table 1.

The star counts and the colour distributions from the stars in the intermediate fields towards the galactic anti-centre are well described with the stellar populations mentioned above. Arguments are given that the actual solar offset is about 15 pc north from the galactic plane.

**Key words:** methods: data analysis – Stars: general, HR-Diagram, statistics – Galaxy: stellar content, structure

### 1. Introduction

Close to the galactic midplane one is most sensitive to stars with a low or moderate scale height. Information about stellar populations from an extended or thick disc can be constrained with observations at high galactic latitudes. The star counts from the north galactic pole field are well suited to disentangle and to determine the scale heights for the various disc populations. The apparent scale height for each spectral type is the cumulative result from different populations with each their own characteristic age, metallicity and scale height. For the determination of the scale heights one should start with the

youngest population with the lowest scale height and proceed backwards to older populations with larger scale heights.

Observational data for the north and south galactic pole (hereafter respectively NGP and SGP) are available from several studies: Weistrop (1972); Faber et al. (1976); Chiu (1980); Kron (1980); Koo & Kron (1982); Gilmore, Reid & Hewett (1985, hereafter GRH85); Murray et al. (1986), Yoshii, Ishida & Stobie (1987); Stobie & Ishida (1987, hereafter SI87); Reid (1990, hereafter RD90); Majewski (1992); Soubiran (1992); and Reid & Majewski (1993, hereafter RM93). In this study the data for the NGP are taken from SI87, RD90, and RM93 and the star counts for the SGP are taken from GRH85.

In the direction of the galactic anti-centre (hereafter GAC) data are available from various sources: Friel & Cudworth (1986) in the direction of  $(l, b) = (175^\circ, -49^\circ)$ , Fenkart & Esin-Yilmaz (1983) and Yamagata & Yoshii (1992, hereafter referred to as YY92) in the direction of  $(l, b) = (200^\circ, 59^\circ)$ , and Ojha et al. (1994, hereafter referred to as OBRM94) for the field towards  $(l, b) = (167^\circ 5', 47^\circ 4')$ . For the analysis we used the data sets from YY92 and OBRM94.

Star counts from Selected Areas (Blaauw & Elvius 1965) and well studied fields are analyzed with the HRD-GST (HR-Diagram Galactic Software Telescope, see Ng 1994 & 1996 and Ng et al. 1995 for details, the latter is hereafter referred to as Paper I). The aim is to generate synthetic CMDs (Colour-Magnitude Diagrams) from first principles, without putting *a priori* observed quantities in the model and to determine in a self-consistent way the structural parameters (scale height, flattening of bulge & halo) and the evolutionary status (age-metallicity) of the stellar populations from fields directed towards the outer part of our Galaxy. The results are used as input for an overall galactic model and are then applied to fields in the direction of the SGP and GAC. In Sect. 2 a description is given of the method used for the analysis. The results are presented in Sect. 3 and they are discussed in Sect. 4.

## 2. Analysis

### 2.1. Method

The stellar population synthesis technique used for the HRD-GST is a powerful tool for the understanding of the complex distribution of stars in CMDs. The different stellar evolutionary phases are linked to each other through libraries with stellar evolutionary tracks. An interpolation is made between sets of evolutionary tracks with different metallicities to obtain a smooth metallicity coverage. With assumptions about the age, metallicity and the shape of the IMF (initial mass function), one obtains information about the star formation history (Bertelli et al. 1992) and the (synthetic) luminosity function.

The MS (main sequence) up to the AGB (asymptotic giant branch) stars from a synthetic population cover a specified age and metallicity range. The mass spectrum is specified with a power-law IMF and the number of stars with a specific age is determined by the SFR (star formation rate). The stars in a particular population all have the same scale height, because they are formed at the same period. High mass stars are only present in (very) young populations, while low mass stars are present in all populations under consideration.

The HRD-GST has thus far been used for the interpretation of the star counts from fields towards the galactic centre (Paper I, Bertelli et al. 1995 & 1996, the first reference is hereafter referred to as Paper II; Ng et al. 1996a, hereafter referred to as Paper III). In Paper I and Ng (1994) it is demonstrated that the age, the metallicity, the scale height of the disc stellar populations and the spatial distribution of the bulge/halo populations (flattening parameter) are the most sensitive parameters. They do not depend critically on the exact choice of the remaining input parameters for which we adopt reasonable values; see Table 1 for the scale length, IMF and SFR. The latter parameters have not been changed throughout the analysis. In this way, the study is simplified and one can focus on the exploration of a limited, but fundamental fraction, of the HRD-GST parameter space. The parameters are determined through an iterative approach: first the most sensitive parameter then the next sensitive and so forth.

The combined data sets from the selected NGP fields span a range of 12 magnitudes in V. We determine the scale heights and age-metallicity for the various stellar populations along the line of sight and apply them to fields towards the SGP and to intermediate latitude fields towards the GAC. It is not possible to obtain stronger constraints for the scale heights and age-metallicity from the latter fields, because they cover a smaller magnitude range. Those fields provide a consistency test and an independent verification of the input parameters from the HRD-GST for an overall galactic model. In all fields the same local normalization is applied (see Sect. 2.3), as determined from the NGP star counts (see Sect. 3.1). Any difference between model and observations is either an imperfection of the model or is due to a local difference in the galactic structure.

### 2.2. Limits

We adopted in the MC (Monte-Carlo) simulations for all fields the following limiting magnitudes:  $B_{lim} = 23^m.5$ , and  $V_{lim} = 22^m.0$ . Differences in the definition of zero-points of the photometric passbands and their transformations result in small colour shifts between the simulated and observed data. Shifts are also induced by differences in age, metallicity or extinction and are considered when a general shift due to a zero-point difference did not remove the observed discrepancy.

The parameters for the HRD-GST determined in this paper are not unique. This makes any test as valid as the most simple test: the MC-simulations goes through all the data points. It has been assumed that young disc populations ought to have higher metallicities and lower scale heights than older ones.

The present mass limit is  $0.6 M/M_{\odot}$  and work is in progress to extend it to lower masses. (Girardi et al. 1996a,b). The absence of synthetic main sequence stars with even lower masses is not a major disadvantage. The missing stars do not contribute to the evolved stars, because they remain on the main sequence for at least a Hubble time. At bright magnitudes, say  $V < 14^m$ , the contribution of low mass stars is negligible. At faint magnitudes, say  $V > 18^m$ , the colour distribution splits up around  $B-V \simeq 1^m.0$  in two parts: a blue and a red distribution (see Fig. 1.3). We have tied our calibration to the blue section, where the low mass stars do not contribute. The presence of low mass stars is not necessary for the determination of the scale heights and the age-metallicities of the disc populations. For the latter a calibration to the blue section is essential.

### 2.3. Normalization

The total mass of the stars within 0.5 kpc along the line of sight is determined for each population. The various populations are then scaled relative to the intermediate disc population (see Table 1). A normalization based on the local mass density in the solar neighbourhood for each population is used here, because it is independent of the assumed passband and detection limit of the simulations. It can eventually be tested against the mass density in the solar neighbourhood. The contribution for each population is obtained by matching through trial and error the observed and the simulated distribution. The following local normalization is inferred for the various stellar populations:  $[\text{halo}/\text{disc}]_{local} = 1/250$ ,  $[\text{bulge}/\text{disc}]_{local} = 1/2850$ ,  $[\text{thick disc}/\text{disc}]_{local} = 4/75$ ,  $[\text{old disc}/\text{disc}]_{local} = 7/18$ , and  $[\text{young disc}/\text{disc}]_{local} = 4.6$ . This normalization has also been applied in the other fields shown in Sect. 3. The normalization above is governed by the local mass density and is not the same as the normalization to the local stellar density from other star counts models.

## 3. Results

Table 1 lists a description of the stellar populations, which are determined with the HRD-GST from mainly the NGP star

**Table 1.** The stellar populations in the HRD-GST determined from the analysis of the star counts towards the North Galactic Pole. It is emphasized that the shapes for the IMF and SFR have been assumed and have not been determined from the star counts data. For all populations a power-law IMF has been adopted with an index  $\alpha = 2.35$ . For the disc populations a scale length of 4.5 kpc is assumed. Better constraints on this value cannot be obtained from this study.

Solar Position:	
Distance from the plane	$45 \pm 5$ pc north <sup>†</sup>
Stellar Populations:	
<i>Halo</i>	
Density law	Power-law with index $n = 3.0$
Axial ratio $q$	1.0
$Z$	0.0004 – 0.003
$t$	16 – 10 Gyr
SFR	Constant
<i>Bulge</i> <sup>††</sup>	
Density law	Power-law with index $n = 3.0$
Axial ratio $q$	1.0
$Z$	0.005 – 0.080
$t$	15 – 13 Gyr
SFR	Exponentially decreasing Characteristic time-scale 2.0 Gyr
<i>Thick Disc</i> *	
Scale height	$1.0 \pm 0.1$ kpc
$Z$	0.0004 – 0.003
$t$	16 – 10 Gyr
SFR	Constant
<i>'Old' Disc</i>	
Scale height	$0.50 \pm 0.05$ kpc
$Z$	0.003 – 0.008
$t$	10 – 7.0 Gyr
SFR	Exponentially decreasing Characteristic time-scale 3.0 Gyr
<i>Intermediate Disc</i>	
Scale height	$0.25 \pm 0.02$ kpc
$Z$	0.008 – 0.015
$t$	7.0 – 4.5 Gyr
SFR	Exponentially decreasing Characteristic time-scale 2.5 Gyr
<i>Young Disc</i>	
Scale height	$0.10 \pm 0.01$ kpc
$Z$	0.015 – 0.020
$t$	5.0 – 1.0 Gyr
SFR	Exponentially increasing Characteristic time-scale 4.0 Gyr
Local Normalization**:	
halo/disc	1/250
bulge/disc	1/2850
thick disc/disc	4/75
old disc/disc	7/18
young disc/disc	4.6

<sup>†</sup> The value for the solar offset determined is too high; 15 pc is a more likely value, see Sect. 4.3 for details.

<sup>††</sup> The parameters have been adopted from Paper II, but its presence is not firmly established from the north galactic pole field.

\* The age of this population is probably about 1 – 3 Gyr too old, see Sect. 4.4.2 for details.

\*\* This normalization is made with respect to the intermediate disc. We normalize to a local mass density, see Sect. 2.3 for details.

counts. A total of six different synthetic stellar populations (halo, 'bulge', thick disc, old disc, intermediate disc, and young disc) are found from the analysis of the NGP data set. The bulge population might not be essential.

### 3.1. The north galactic pole

NGP:  $l = 81^\circ 0$ ,  $b = +87^\circ 0$  & SA 57:  $l = 65^\circ 5$ ,  $b = +85^\circ 5$

The surveys from SI87, RD90, and RM93 cover an area of respectively 21.46 degree<sup>2</sup>, 28.3 degree<sup>2</sup> and 0.29 degree<sup>2</sup>. Majewski (1993) pointed out that a gradient in the magnitude scale as large as  $0^m.25$  is present in the Chiu (1980) magnitudes. This gradient is probably caused by systematic errors in the old iris photometry. Because RD90 based his photometric calibration on the Chiu (1980) magnitudes, systematic errors can be present in the photometry.

In the analysis the following offsets in (B–V) are adopted in the MC simulations:  $+0^m.05$  and  $-0^m.05$  (+ refers to a blue shift of the MC distribution) for respectively SI87 and RM93. In the data set from RD90 a small gradient is present, resulting in a (B–V) shift of  $+0^m.15$  for  $V = 13^m - 14^m$  and  $+0^m.05$  for  $V = 18^m - 19^m$ . An offset of  $+0^m.10$  is adopted in Fig. 1.2.

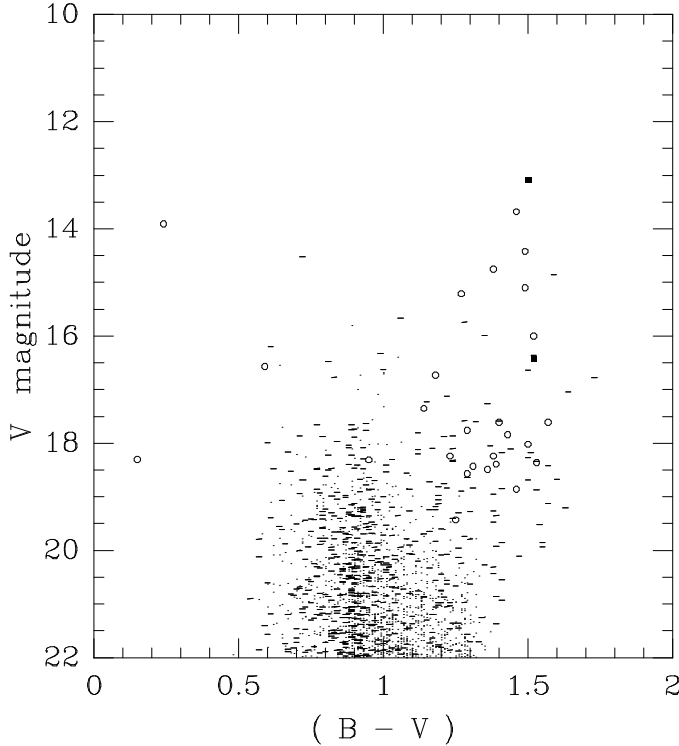
For the NGP we adopted  $E(B-V) = 0^m.0$ . For the simulations of the photometric errors the following values are used over the whole magnitude range of interest:  $\sigma(B) = 0^m.02$  and  $\sigma(V) = 0^m.02$  for the RM93 star counts,  $\sigma(B) = 0^m.05$  and  $\sigma(V) = 0^m.05$  for the SI87 star counts, and  $\sigma(B) = 0^m.10$  and  $\sigma(V) = 0^m.10$  for the RD90 star counts. Comparable errors need to be adopted in the MC-simulations, otherwise a comparison with the observations is meaningless.

In Figs. 1.1 – 1.3 the colour distributions from respectively SI87, RD90 and RM93 are compared with the MC simulations. In figure 1.1a it is noted that the MC simulation over-predicts considerably the number of evolved stars around  $B-V = 1^m.2$ . Inspection of the stars brighter than  $V = 12^m.5$  in SI87's CMD (their Fig. 7) shows, that the stellar locus becomes gradually bluer towards brighter magnitudes. This could be due to the presence of even younger stars, but also due to systematic errors in the calibration of bright stars. The latter moves the bright evolved stars into the bluer stellar locus.

Figure 2.0 shows the combined CMD of the six stellar populations considered. Figures 2.1, 2.2, 2.3, 2.4, 2.5, and 2.6 display the individual CMDs, respectively young disc, intermediate disc, old disc, thick disc, bulge, and halo. Table 1 gives a description for each population. Figure 2.7 shows the CMD for the halo contribution when the  $R^{1/4}$ -law is used. The simulations in Figs. 2.0 – 2.7 represent an area of about 5.0 degree<sup>2</sup>. In Figs. 2.1 – 2.4 the sharp cutoff of the MS (main sequence) due to the lower mass limit of the evolutionary tracks in the HRD-GST is clearly visible. Note that this cutoff becomes redder, when going from an old and metal-poor population (Fig. 2.4) to younger metal-richer populations (Figs. 2.3 – 2.1). From Fig. 2.4 it is seen that the thick disc contribution becomes negligible for  $B-V \simeq 0^m.5$  and  $V > 18^m$ . At this colour and magnitude the stellar contribution can only be due to halo

stars. A point of attention is that the current description of the halo population does not provide blue horizontal branch stars (see Fig. 2.6). These stars can be generated by lowering the metallicity or adopting an older age. The latter shifts the main sequence and the core H-exhausted stars to redder colours and increases the discrepancy even more. Therefore, an older age for the same metallicity range can be ruled out and the lower metallicity limit of the halo population should most likely be decreased. In this case a slightly older age is allowed.

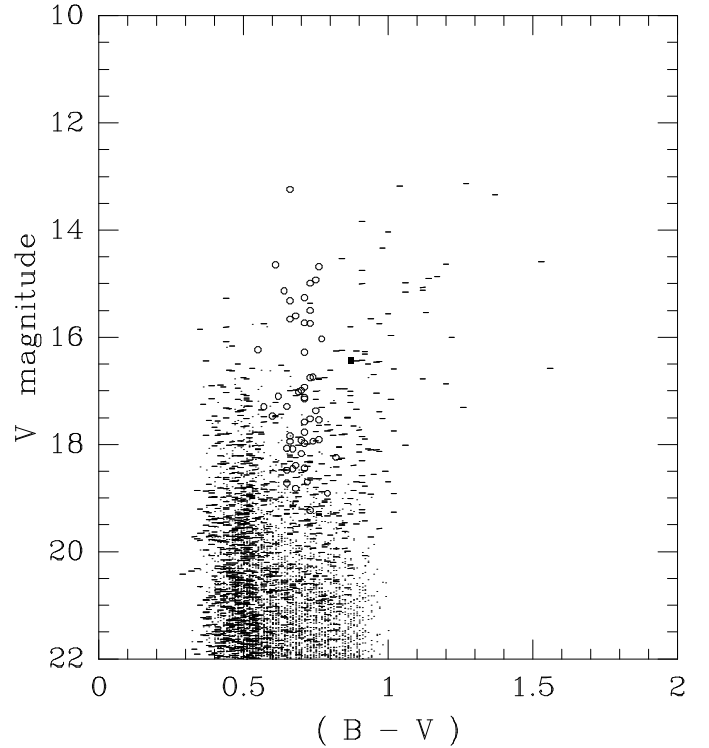
Figure 3.1c shows from the MC simulations the resulting bolometric luminosity function for stars in the spheroid (Fig. 3.1a) and in the disc (Fig. 3.1b) component.



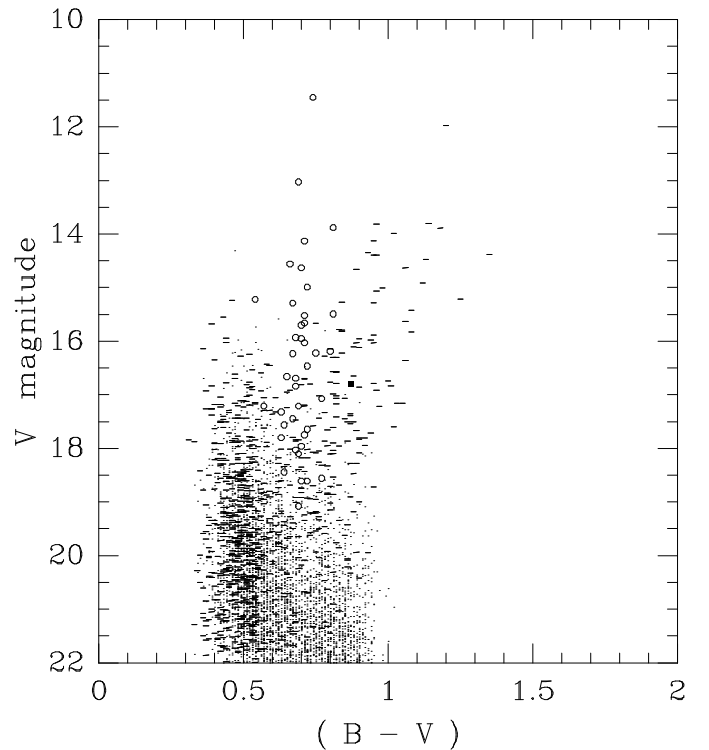
**Fig. 2.5.** Simulated (V,B-V) CMD for the bulge population in the direction of the NGP, see figure 2.0 for the symbols and table 1 for details

Figure 3.2c shows the resulting star counts from the MC simulations in the spheroid (Fig. 3.2a) and in the disc (Fig. 3.2b), together with the observed star counts from SI87 (filled dots) and RM93 (open dots). From this figure it is evident that up to  $V=18^m0$  the majority of the observed stars are disc stars. The stars in the spheroid become important for  $V > 18^m0$ . In Figs. 1.2d, 1.2e, 1.3a, and 1.3b it can be seen that the HRD-GST model over-predicts the number of observed stars, while low mass main sequence stars with  $B-V > 1^m4$  are lacking. In the star counts (Fig. 3.2b) one notices that these differences cancel each other out. One cannot rely solely on the goodness of star counts fits. An inspection is required of the colour distributions and/or the synthetic CMD.

Figure 3.3c gives the total number of simulated stars detected in the line of sight through the spheroid (Fig. 3.3a)



**Fig. 2.6.** Simulated (V,B-V) CMD with a power-law for the halo population in the direction of the NGP, see figure 2.0 for the symbols and table 1 for details



**Fig. 2.7.** Simulated (V,B-V) CMD with the  $R^{1/4}$ -law for the halo population in the direction of the NGP, see figure 2.0 for the symbols and table 1 for details

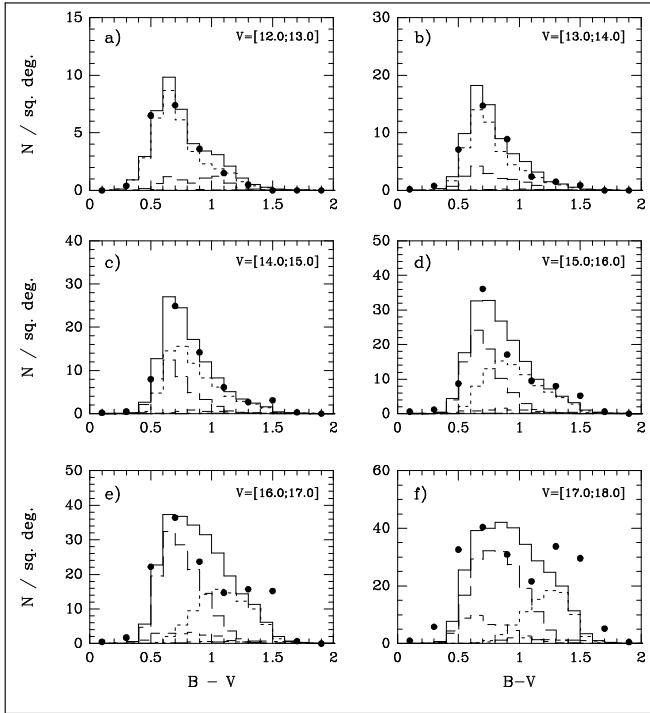


**Fig. 4.1.** Colour distribution from Gilmore, Reid & Hewett (1985, filled dots) in the direction of the SGP; see text and Fig. 1.1 for additional details

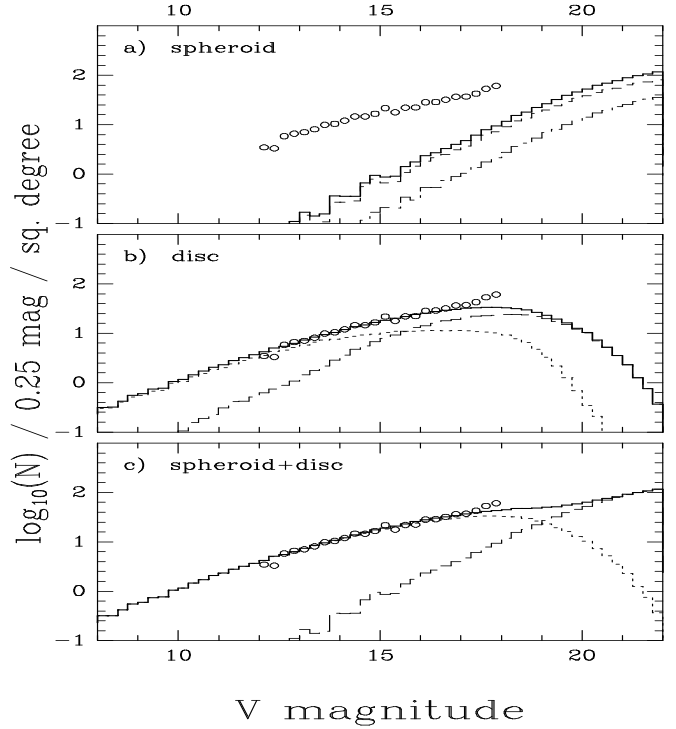
and the disc (Fig. 3.3b). This and the next figure suggest, that there are some nearby ( $d < 250$  pc) stars missing in the disc of the HRD-GST model. One would expect in the local solar neighbourhood a gradually increasing or flat curve, but not a decreasing one. The discrepancy originates from stars with masses  $M/M_{\odot} < 0.6$ . Notice that there is no dip at the disc/spheroid transition.

Figure 3.4c gives the total mass, including those below the detection limit, from stars with  $M/M_{\odot} > 0.6$  in the line of sight in the spheroid (Fig. 3.4a) and in the disc (Fig. 3.4b).

### 3.2. The south galactic pole

For the SGP we used the GRH85 star counts, covering an area of  $18.2 \text{ degree}^2$ . For the MC simulations we found after trial and error:  $E(B-V) = 0^m 00$ ,  $\sigma(B) = 0^m 05$  and  $\sigma(V) = 0^m 05$ . There is no apparent offset present between the observed and simulated  $(B-V)$  colour distributions. But it is possible, that the reddening and the offset cancel each other out.

Figure 4.1 shows the comparison of the SGP data with the HRD-GST predictions. Figure 4.2c shows the resulting star counts from the MC simulations in the spheroid (Fig. 4.2a) and in the disc (Fig. 4.2b), together with the observations. The GRH85, YY92 and OBRM94 star counts are mainly due to disc stars. One has to be cautious, because it is not possible to determine the flattening of the spheroid from these data sets.



**Fig. 4.2.** Star counts from the MC simulations shown in Fig. 4.1. Open dots are the star counts from GRH85, see captions of the Figs. 1.1 & 3.1 for additional details

### 3.3. Intermediate latitude fields

3.3a.

$$\text{SA 54: } l = 200^{\circ}1, b = +58^{\circ}8$$

The source of the data for SA 54 is YY92. Their study covered an area of  $16 \text{ degree}^2$ . For the MC simulations we adopted:  $E(B-V) = 0^m 08$ ,  $\sigma(B) = 0^m 10$  and  $\sigma(V) = 0^m 10$ .

Figure 5.1 shows the comparison of observational data from YY92 with the HRD-GST. In Figs. 5.1a & 5.1b the colour distributions predicted by the HRD-GST are shifted respectively  $0^m 20$  and  $0^m 05$  blueward in Figs. 5.1a and 5.1b. The origin of this shift is probably caused by a calibration error, due to saturation effects of stars brighter than  $V = 12^m$ . Additional observations in independent directions are required to confirm this. Because it might on the other hand, not be due to systematic photometric errors. Exactly the same shift is present in the colour distribution from OBRM94, who used comparable photographic material in their study. Figure 5.2c shows the resulting star counts from the MC simulations in the spheroid (Fig. 5.2a) and in the disc (Fig. 5.2b), together with the observations.

3.3b.

$$l = 167^{\circ}5, b = +47^{\circ}4$$

The source of the data for this field is OBRM94. Their study covered an area of  $18.8 \text{ degree}^2$ . For the MC simulations the values for the reddening and photometric errors are the same as those adopted for YY92.

Figure 6.1 shows the comparison of the OBRM94 data with the HRD-GST predictions. In Figs. 6.1a & 6.1b the colour distributions predicted by the HRD-GST are shifted respectively

$0^m20$  and  $0^m05$  blueward. Figure 6–2c shows the resulting star counts from the MC simulations in the spheroid (Fig. 6.2a) and in the disc (Fig. 6.2b), together with the observations.

A comparison of Fig. 6.2 with Fig. 10 from OBRM94 shows that the HRD-GST model basically covers the whole magnitude range of interest, while the Besançon model over-predicts the number of stars in their Fig. 5 at  $V < 13^m$ . The origin of this is not clear, because the (B–V) distributions for  $V < 13^m$  are not displayed by OBRM94. Possibly the contributions from the young and intermediate disc populations have been slightly over-estimated in the Besançon model, because relative higher weights are given to the  $V > 13^m$  magnitude bins. A comparison between OBRM94’s Fig. 11a with our Fig. 6.1d shows that the HRD-GST under-predicts the colour distribution slightly, while the Besançon model is in good agreement. The discrepancy with the HRD-GST predictions is caused by the relative normalization between the young and intermediate disc.

## 4. Discussion

### 4.1. Age and metallicity

The stellar populations from the disc and spheroid have been successfully used in star counts studies in different directions in our Galaxy. The same local normalization is used for all fields. No deviations have been found, which are directly related with metallicity differences in one of the stellar populations.

Figure 7 shows the age-metallicity relation for the disc populations listed in Table 1. This relation decreases in metallicity to old age. Freeman (1992) demonstrated with the Edvardsson et al. (1993) sample of F-stars that there is no apparent evidence for a gradient in the age-metallicity relation. There is mainly a large scatter in metallicity at a particular age. However Edvardsson et al. (1993) used the Vandenberg (1985) isochrones to determine the ages. Those isochrones were computed with opacities derived from the LAOL (Huebner et al. 1977) element mixes. Significant changes in the ages of intermediate to solar metallicity stars are expected, when they are derived from isochrones computed with the radiative opacities derived from OPAL (Rodgers & Iglesias 1992, Iglesias et al. 1992). At  $Z=0.001$  there is virtual no age difference between the isochrones computed with LAOL or OPAL based opacities (Bertelli et al. 1994). Towards higher metallicities the ages will be progressively younger. The flat age-metallicity relation might be an artifact of LAOL based isochrones. At present the situation is not clear and a revision of the ages from the Edvardsson et al. data set is required with OPAL based isochrones to solve this ambiguity.

In the radial direction there is apparently no metallicity gradient within a population, which is in agreement with the suggestions obtained from B-stars (Kaufer et al. 1994, Prantzos & Aubert 1995). Due to their short lifetimes, B-stars can be considered as one population. On the other hand, Carraro & Chiosi (1994) and Piatti et al. (1996) showed with young open clusters that there is a radial metallicity gradient.

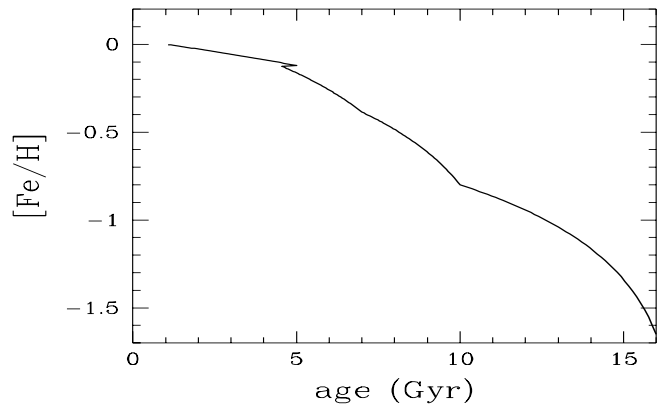
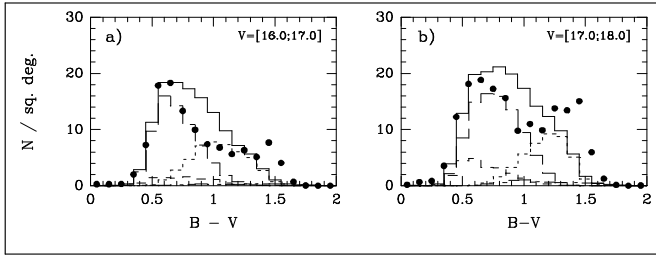


Fig. 7. The age-metallicity relation for the disc populations in Table 1

If one samples from a young to an older population and if the scale length is the same for all populations one would find no metallicity gradient. On the other hand, an inter-population metallicity gradient should be present when the various disc populations do not have the same scale length. The direction of this gradient is directly related with an increasing or a decreasing disc scale length towards younger stellar populations. The metallicity gradient from planetary nebulae (Maciel & Koppen 1994 and references cited therein) might have its origin in a mix of the disc populations and it could be an indication for a different scale length of these populations. An independent indication that this is the case comes from open clusters (Paper III), which gives  $h_0 = 2.3 + 0.12 t_9$  kpc ( $t_9$  the age of the population in Gyr). The scale length determined for the young & thick disc component, respectively  $2.5 \pm 0.3$  kpc (Robin et al. 1992) &  $2.8 \pm 0.8$  kpc (Robin et al. 1996) or  $2.3 \pm 0.6$  kpc &  $3.8 \pm 0.5$  kpc (Ojha et al. 1996), provide another indication. The 2.8 kpc scale length from Robin et al. (1996) is probably too small. It is based only on the field towards the galactic centre, while their parameter space towards the GAC field appears to be degenerate (see the likelihood contours in their Figs. 5a–d). Our results favour the presence of a radial metallicity gradient induced by the subtle difference of the scale length of different stellar populations.

Perpendicular to the galactic plane the following situation occurs: within a particular disc population there is no metallicity gradient, while sampling from young (relatively nearby) to older (relatively far away) populations will give rise to a vertical metallicity gradient. This gradient might be stronger than the radial gradient and is in fact in agreement with the results found by Piatti et al. (1996). These results do not contradict the result obtained by Carraro & Chiosi (1994). They found no evidence for a vertical gradient after correction of the radial gradient, i.e. they found no gradient within a population.

The different ages of the stellar populations in the disc are not merely an empirical match to the observations. It has been observed in the distribution of open clusters in the galactic plane. The  $\delta V$  distribution of open clusters from Phelps et al. (1994) shows an almost flat distribution with two distinct peaks at the end of each side. The index  $\delta V$  is an age parameter and is



**Fig. 8.** Colour distribution for stars with  $V=16^m0-18^m0$  from Stobie & Ishida (1987: filled dots) in the direction of the NGP, see Fig. 1.1 for additional details

defined as the magnitude difference between the MS turn-off and the RHB. Probably the peaks are related with the occurrence of two burst during the formation of the disc. The ages of these clusters (Carraro & Chiosi 1994; Phelps et al. 1994) show that these peaks correspond with burst between 7–6 Gyr and 2–1 Gyr. The peak between 7–6 Gyr corresponds with the start of the formation of the intermediate disc. The peak between 2–1 Gyr is related to the formation of the young disc population.

#### 4.2. Initial mass function

The colour distributions from RD90 (Figs. 1.2d & 1.2e), RM93 (Figs. 1.3a & 1.3b), SI87 (Figs. 8a & 8b) and GRH85 (Figs. 4.1e & 4.1f) show a systematic discrepancy between the observed and the modeled ( $B-V \gtrsim 0^m7$ ) colour distributions. The origin of this difference resides inside the HRD-GST, because the observations are from independent sources. From Figs. 2.1–2.3 it can be seen that this is due to the MS from the disc stars. Apparently there are too many MS stars generated with  $M/M_{\odot} < 1.0$ . This contributes partly to the discrepancy noted between the observed and the simulated colour distributions in Paper I. We adopted a slope  $\alpha = 2.35$  for the power-law IMF. The results from Kroupa et al. (1993) show that this is a reasonable value for the mass range considered here ( $M/M_{\odot} > 0.6$  to the main sequence turn-off mass at a particular age). The present work indicates that the slope of a power-law IMF near the HRD-GST mass limit is flatter than the slope near the main sequence turn-off. This is in agreement with the decrease in the IMF slope expected on theoretical grounds (Richtler 1994 and references cited therein).

#### 4.3. The solar offset

Since the early Sixties, the asymmetry in the distribution between the NGP and SGP has been ascribed to the solar position in the plane. The general trend is that an offset, ranging from 5–40 pc, north of the galactic plane has been found (Cohen 1995; Humphreys & Larsen 1995; Paper I).

There would be no difference between the NGP & SGP data set, if the Sun is located exactly in the galactic midplane. A comparison of the model predictions and the observations between these fields show some differences, which is likely

due to the solar offset. Discrepancies between the NGP & SGP is then minimized by putting the Sun with 10 pc steps out of the galactic plane. The SGP & NGP data sets from respectively GRH85 and SI87 have been used, because they have comparable photometric errors. An integral approach was made, but emphasis is put on the bright stars ( $V < 14^m0$ ) in these fields. With this procedure a determination was made of the displacement of the Sun from the galactic plane and an offset  $45 \pm 5$  pc north from the galactic plane is obtained. This is higher than the generally accepted value around 15 pc (Conti & Vacca 1990, Cohen 1995, Hammersley et al. 1995, Binney et al. 1996). On the other hand, it is remarkably similar to the values obtained by SI87 and YY92. The data sets used for this determination are in fact the same, but different methods are used. The large value is probably due to systematic differences in an heterogeneous data sets. For example, small differences in the zero point between the photometric systems or their transformations to the standard Johnson B & V magnitudes might be responsible for the high offset. For a better determination of the offset a homogeneous data set ought to be preferred. In a photographic survey Humphreys & Larsen (1995) find from such a data set a lower value for the solar offset. With a scale height of 350 pc they obtained  $20.5 \pm 3.5$  pc. Humphreys & Larsen (1995) over-estimated the scale height of the major disc component, which is 250 pc (Kent et al. 1991, Ng 1994, Papers I & III). In that case, they would have obtained with their Fig. 6 a value of about 15 pc.

The different methods all converge to an offset of about 15 pc north from the galactic plane when a homogeneous data set is used. It is therefore even more striking that  $13.5 \pm 1.9$  pc was found by van Tulder (1942) from detailed studies of the distributions of various types of stars. It is concluded that the solar offset is around 15 pc. It is stressed that this result does not influence any of the other results presented in this paper, because this effect is small on the stars from the old and thick disc population. This offset is important though in the studies of (very) young stars in the galactic plane.

#### 4.4. Stellar populations in the disc

In Paper I it is found, that at low latitudes the dominating populations must be of intermediate to young age. For these populations a scale height of respectively 250 pc and 100 pc is found. From the analysis of the NGP data these results are confirmed. The population with a scale height of 500 pc in our analysis is called the old disc. At high galactic latitudes a fourth metal-poor population with a 1.0 kpc scale height is found. This population is hereafter referred to as the thick disc.

##### 4.4.1. The old disc population

From the analysis of *ubvy* $\beta$  CCD photometry of stars brighter than  $V=20^m$  in a field ( $l=262^\circ$ ,  $b=4^\circ$ ) close to the galactic plane Jønch-Sørensen & Knude (1994) found a separate population of stars. At a distance of about 10 kpc, about 700 pc above the plane, a significant number of these stars are found. The age

and chemical composition of these stars are well represented by an 8 Gyr isochrone with  $[\text{Fe}/\text{H}] = -0.47$  ( $Z \simeq 0.005$ ). According to Jønch-Sørensen & Knude (1994) these stars are part of the so-called extended disc (Majewski 1993). The contribution from stars with a scale height of 1.4–1.6 kpc (RM93) in the extended/thick disc population is expected to be the dominant population, starting at about 20 kpc distance along the line of sight of this field. The stars in question though are located at half this distance. The age and metallicity are furthermore in good agreement with, what is called in this paper, the old disc population, which has a scale height of 500 pc. Therefore, the population identified by Jønch-Sørensen & Knude (1994) is strongly related with our old disc population. The results from Paper III ( $l = 1^\circ 0$ ,  $b = -3^\circ 9$ ) indicate that a small feature near  $V-I \simeq 1^m 2 - 1^m 4$  and  $V = 19^m$  in the CMDs is related with the MS turn-off of this disc population. The consistency between fields in different directions in the galactic plane are an indication that the old disc population is distinct in age-metallicity and scale height.

#### 4.4.2. The age-metallicity of the thick disc

In Figs. 1.2e, 1.2f, 1.3b, and 1.3c it is noted that the colour distributions from the MC simulations do not match the observed distributions at  $B-V < 0^m 3$ . Because this trend is present in two independent data sets it must be a real feature, which is not covered properly by the HRD-GST. Part of the shift in Figs. 1.2e & 1.2f is due to the gradient in the magnitude scale (Sect. 3.1). This trend is visible at  $V > 18^m$  and is due to the halo or the thick disc (see Figs. 2.1–2.6).

The evolutionary tracks in the HRD-GST do not extend to metallicities lower than  $Z = 0.0004$ . A metallicity  $Z < 0.0004$  will not account fully for the discrepancy, because this will only shift a small number of HB (horizontal branch) stars to bluer colours. One should be aware, that due to the metallicity range and the implicit linear age-metallicity relation in the HRD-GST (Paper I), the majority of the stars have metallicities larger than  $Z = 0.0004$ . Therefore, the origin for this discrepancy must be due to the age of one or both populations. If the halo population is younger, the simulated distributions at fainter magnitudes (frames d, e, and f from Fig. 1.3) becomes bluer. The observed distributions do not allow this. Therefore, the thick disc population is likely younger than assumed. An upper limit for the age in the interval 13–16 Gyr is well possible. Such an age gives a small contribution of ‘blue’ stars between  $16^m < V < 18^m$ . It is not clear though if this removes completely the discrepancy between  $18^m < V < 19^m$ .

The metallicity of the thick disc is a controversial issue. Morrison et al. (1990) found from metallicity ranking with DDO photometry evidence for a metal-poor tail. The spectroscopic results from Ryan & Lambert (1995) on a sample of stars, classified as metal-poor with DDO photometry, contradict this, but they lack the data to confidently reject the presence of metal-poor stars in a thick disc. Their sample is formed by giant stars with  $V$  magnitudes spanning the range  $8^m 0 - 12^m 0$  and  $B-V$  colours ranging roughly from  $0^m 75 - 0^m 95$ . Figures

2.2–2.4 show that with these criteria virtually no metal-poor stars from the thick disc would have entered their sample. Their result mainly demonstrate that metallicity ranking with DDO photometry is not reliable towards low metallicities.

Beers & Sommer-Larsen (1995) performed a larger spectroscopic study and found convincing evidence for a metal-poor tail for the thick disc down to at least  $[\text{Fe}/\text{H}] = -2.0$ . They selected a large variety of stars (MS, RGB, HB and AGB stars), covering a large magnitude interval. Their study does not contain the selection bias as in the study from Ryan & Lambert. In conclusion: our findings for a metal-poor thick disc are in agreement with the results from Beers & Sommer-Larsen.

#### 4.4.3. The thick disc population: scale height

The metal-poor thick disc is identified from the excess of stars at the blue edge ( $B-V \simeq 0^m 4$ ) of the colour distributions in Figs. 1.2d, 1.2e, 1.3a & 1.3b. The parameters found here are different from those obtained with the Besançon model (Robin et al. 1996, Ojha et al. 1996). Their thick disc parameters are  $z_0 = 760 \pm 50$  pc and  $[\text{Fe}/\text{H}]$  ranging from  $-0.6$  to  $-0.9$  or  $Z \simeq 0.003 - 0.005$ . These values are intermediate to the parameters determined for our old and thick disc population. Their metallicity is close to our transition metallicity between the two populations. From our work we expect, that the age of their thick disc population is close to 10 Gyr.

The difference in the results originates from the initial conditions between the two models. The Besançon model adopts a vertical age-velocity dispersion. In suitably chosen age-velocity bins the scale heights are calculated from the galactic potential (Bienaymé et al. 1987). These disc sub-populations are then fitted to the observations and the thick disc is obtained from the stars not fitted by these sub-populations. We explored the parameter space through a direct comparison between the observed and the synthetic distribution. The age-metallicities and scale heights of the populations described in this paper are not expected to coincide exactly with the selection of age-metallicity bins selected for the Besançon model. Our results are therefore complementary with those obtained with the Besançon model. This explains why their thick disc scale height can be intermediate to our old and thick disc value, but this does not explain the actual value.

About half of the star counts surveys used by Robin et al. (1996) are complete up to about  $V = 18^m$ . At this magnitude a disc population will have a scale height intermediate to our old and thick disc (see Figs. 2.3 & 2.4), i.e.  $z_0 \simeq 750$  pc. For a small number of data sets the limiting magnitude was brighter than  $V = 18^m$  and these data sets cannot be used to constrain a disc population with  $z_0 \gtrsim 750$  pc. Only the RM93 data set is reliable to magnitude limits fainter than  $V = 18^m$ , but the results obtained by Robin et al. from this field could be biased by the results obtained from the other fields. The scale height for the thick disc obtained by Robin et al. (1996) is likely induced by the completeness limits of the data sets analyzed by them.

The parameters for the thick disc population listed in Table 1 are not very different from those given by YY92. They



obtained 900 pc, which is within the estimated uncertainty of our population. It is not clear though if the scale height is comparable with the 1170 pc thick disc parameterized by Chen (1996), but the scale height is within the uncertainties of the  $1140 \pm 60$  pc obtained by Spagna et al. (1996).

#### 4.4.4. Indications for a possible merger

The simulations from Mihos & Hernquist (1996) indicated that ‘major’ mergers, between galaxies with comparable mass, should produce objects resembling ellipticals. Quinn et al. (1993) show that a merger event with galaxies comparable to the LMC and SMC could destroy the parent disc. Unavane et al. (1996) demonstrated quantitatively, that a merger scenario is not likely between our Galaxy and a LMC or SMC type galaxy. If a merger event had occurred, it should have been with a galaxy with a mass comparable to those from dwarf ellipticals. Walker et al. (1996) show that ‘minor’ merger events with dwarf elliptical satellites do not destroy the parent disc and that they could puff up part of the disc by  $\sim 60\%$ . It is not clear, if the puffed up part of the disc forms a layer on top of the parent disc. And if this layer is in age-metallicity and scale height distinct from a hierarchical formation process. Walker et al. argue that other arrangements are certainly possible with the parameters available to twiddle the simulations. Their work provide indications about general aspects of merger events. Detailed numerical inference from these simulations should be avoided, because the results depend sensitively on the choice of scale parameters.

A minor merger event could move some stars from the metal-poor disc population with a 1 kpc scale height to roughly a 2 kpc scale height. The RR-Lyrae stars from a flattened component with a 2 kpc scale height from Kinman et al. (1994) could be a record from a fossil merger event. The RM93 thick disc is possibly another record of a minor merger event. The 1.2–1.4 kpc scale height is larger than the 1.0 kpc scale height for the metal-poor thick disc component discussed in Sects. 4.4.2 & 4.4.3. On the other hand, the colours of the stars from the RM93 thick disc are redder. It is important to determine how the RM93 thick disc stars are related in age and metallicity with a population intermediate to the populations with a 0.5 kpc and 1.0 kpc scale height from our work. This provides an indication on when a minor merger event could have occurred with our Galaxy.

#### 4.4.5. Low mass stars

The effect of the  $0.6 M/M_{\odot}$  mass limit (stars with smaller masses are hereafter referred to as low mass stars) in the HRD-GST is that the features with  $B-V > 0^m.95$  in Fig. 1.3f to  $B-V > 1^m.35$  in Figs. 1.1f & 1.3a are not covered by the MC simulations. However, the synthetic CMDs give indications on the contribution of the low mass stars. Figs. 2.1–2.4 indicate that the small number of missing stars red stars in Figs. 1.1f & 1.3a are related to the young disc population with a 100 pc scale height, while the missing stars in Figs. 1.3b & 1.3c are due to the combined contribution of low mass stars from populations

with a scale height of 100 pc, 250 pc and 500 pc. The low mass stars from populations with a 500 pc and 1.0 kpc scale height are the main contributors at  $V > 20^m$  and  $B-V > 0^m.95$ . The cumulative distribution of the low mass stars can be used to constrain the IMF down to the hydrogen burning main sequence mass limit in a similar way as discussed in Sect. 4.2 for stars with  $M/M_{\odot} > 0.6$ . Only in this way, mixes of stellar populations with different scale heights, ages and metallicities are taken properly into account. According to Mera et al. (1996) the slope  $\alpha = 2.0 \pm 0.5$  for the power-law IMF for stars with  $M/M_{\odot} < 0.5$ , while Kroupa et al. (1993) and Tinney (1995) find a considerable smaller value.

#### 4.5. Stellar populations in the spheroid

In the spheroidal component two populations are distinguished. The first is easily identified with the metal-poor halo population. The age range of the halo stars is comparable with the 5–7 Gyr age range from the bulk of halo globular clusters (Chaboyer et al. 1996). The second is a metal-richer bulge population. Its presence is not established unambiguously from this study. The parameterization adopted here is taken from Paper II, which differs from Paper III, mainly in the upper metallicity limit. It is not clear though whether the difference between Paper II & III is caused by an outward, radially decreasing metallicity gradient. Not enough fields have been analyzed thus far, but the work from Minniti (1995 and references cited therein) appears to support this. Both populations reside in the spheroid, which is barely or not flattened.

##### 4.5.1. Flattening of the spheroid

The hitherto supposed flattening of the spheroid is likely due to mixtures of the metal-poor halo with the thick disc stars. The flattening of the spheroid is very small ( $0.95 < q < 1.00$ ). A negligible amount of flattening has already been noted in the distribution of halo globular clusters (Zinn 1985). The colour distribution is not matched properly with a power-law at  $V > 20^m$  for a stronger flattening, which would disperse the halo stars over a larger magnitude range. This is no in agreement with the more concentrated distribution of the halo stars.

A duality in the distribution of metal poor stars has been suggested by Hartwick (1987) from the analysis of the density distribution of RR Lyrae stars. Similar results are obtained by Norris (1994) and Kinman et al. (1994). An extensive discussion of this duality is given by Norris (1994 and references cited therein). He finds in high proper motion samples of MS stars two distinct components: the halo and the so-called metal-poor thick disc (Morrison et al. 1990) with  $-3.0 \leq [\text{Fe}/\text{H}] \leq -1.0$ . These values are consistent with the metallicity range  $Z = 0.0004 - 0.003$  obtained from the analysis of the NGP star counts with the HRD-GST (taking into account that in the current setup of the HRD-GST the lower metallicity limit is  $Z = 0.0004$  and that the upper limit can be in the range  $Z \simeq 0.001 - 0.005$ ). A consequence of this duality is that RR Lyrae stars are expected in both the halo and the

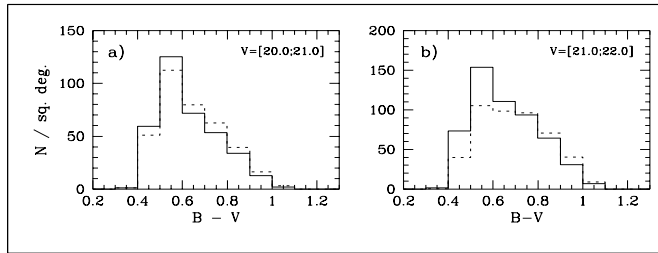


**Fig. 9.** Colour distribution for synthetic stars from the halo population in the magnitude interval  $V = 20^m 0 - 22^m 0$ , described by a power-law (solid line) and a  $R^{1/4}$ -law (dashed line) in the direction of the NGP

thick disc. A sample of supposed halo RR Lyrae stars can be polluted with stars from the thick disc. Therefore, Wesselink (1987) might have overestimated the amount of flattening from his sample of RR Lyrae stars, presumably located in the halo.

Our results support the notion that an overlap is present in the age and chemical composition of the halo and thick disc populations. They indicate that the classical flattening parameter in star counts models needs a revision. Star counts studies towards other deep fields towards the galactic poles are required to verify this.

#### 4.5.2. Power-law or $R^{1/4}$ -law

In contrast to a power-law with index  $n=3.0$ , the MC simulations show that the  $R^{1/4}$ -law, as parameterized by Bahcall & Soneira (1984), does not give for  $V > 20^m$  the proper distribution. In particular for the stars with  $B-V \simeq 0^m 5$ , where the density starts to drop significantly with a  $R^{1/4}$ -law. In Figs. 9a & 9b the two distributions are compared with each other. They show that a halo population described with the  $R^{1/4}$ -law predicts at fainter magnitudes less stars with respect to a power-law description. This drop in density cannot be fully compensated by adopting a stronger flattening, because the drop in the  $R^{1/4}$ -law is mainly driven by the exponential in this expression. Although the number of stars are considerably smaller, a similar discrepancy is visible in a comparison between the star counts ( $I = 23^m - 25^m$ ) and a galactic model that utilizes the  $R^{1/4}$ -law for the description of the halo (Mould, 1996). Differences are notably also present in the distribution of the RGB (red giant branch) stars with  $B-V > 1^m 0$ .

#### 4.5.3. Metal-rich stars

The contribution of the halo becomes noticeable at  $V > 18^m$  (see figure 1.3c and 2.6). At  $V > 21^m$  the width of the  $B-V$  colour distribution between  $0^m 4$  to  $1^m 0$  is too wide for halo stars only. There is a contribution missing between  $0^m 8 \lesssim B-V \lesssim 1^m 0$ . The contribution from the old and thick disc population (see Figs. 2.3 & 2.4) is not sufficient to explain this. This missing stars must be fairly old, because any population which is significant younger becomes not only bluer, but also gives a larger contribution at magnitudes brighter than  $V = 20^m$ . An additional contribution could be due to metal-

rich stars from an old population. The numerical calculations from Steinmetz & Müller (1995) suggest the presence of some metal-rich stars in the outer parts of the Galaxy. In the simulations a population similar to the metal-rich population found in Paper II is adopted. Figure 1.3f shows, that the inclusion of this population gives a better agreement between the MC simulations and the observations. The presence of metal-rich stars cannot be unambiguously established, but on the other hand it cannot be excluded. This shows that the metal-rich stars are not dominantly present in the outer parts of the Galaxy.

## 5. Conclusions & future work

We studied the colour distribution towards the galactic poles and anti-centre. The analysis shows that the distributions are well reproduced by the sum of four stellar populations in the disc: a young, intermediate, old, and thick disc population.

In the spheroid two major populations are distinguished: a metal poor halo population and a metal richer ‘bulge’ population. The presence of the latter could not be well constrained from the north galactic pole observations. Both the halo and the bulge are well described by a power-law with index  $n=3.0$ . Furthermore, the spheroid appears not to be flattened or the flattening is very small ( $0.95 < q < 1.00$ ).

There are still some discrepancies present between the model and the observed colour distributions. These discrepancies are related with the decrease of the slope of the power-law IMF for stars with  $M/M_{\odot} < 1.0$  and the age of the thick disc stars. They might bias the local normalization. Therefore, the IMF will be the subject for future research, where the lower mass limit in the HRD-GST library of stellar evolutionary tracks is extended downwards to  $0.15 M_{\odot}$ . With an improved galactic model the HRD-GST might be able to obtain better constraints for the bulge population and to distinguish between stellar populations from a hierarchical formation process or those from a merger event.

*Acknowledgements.* Dr. A. Blaauw is thanked for his helpful & critical notes on Chapter 8 of Ng’s Ph.D. thesis. This is a revised and updated version of this chapter. Ng acknowledges J. Lub and D.K. Ojha for helpful discussions & comments and M. Cohen, A. Koekemoer, N. Reid and A.C. Robin for their suggestions. G. Bertelli, A. Bressan and C. Chiosi acknowledge the financial support received from the Italian Ministry of University, Scientific Research and Technology (MURST) and the Italian Space Agency (ASI). Ng acknowledges the financial support, received at the IAP-CNRS, from HCM grant CHRX-CT94-0627 from the European Community.

## References

- Bahcall J.N., Soneira, R.M., 1984, ApJS 55, 67
- Beers T.C., Sommer-Larsen J., 1995, ApJS 96, 175
- Bertelli G., Mateo M., Chiosi C., Bressan A., 1992, ApJ 388, 400

- Bertelli G., Bressan A., Chiosi C., Fagotto F., Nasi E., 1994, *A&AS* 106, 275
- Bertelli G., Bressan A., Chiosi C., Ng Y.K., Ortolani S., 1995, *A&A* 301, 381 (Paper II)
- Bertelli G., Bressan A., Chiosi C., Ng Y.K., 1996, *A&A* 310, 115
- Bienaymé O., Robin A.C., Crézé M., 1987, *A&A* 180, 94
- Binney J., Gerhard O., Spergel D., 1996, *MNRAS* *submitted* (astro-ph/9609066)
- Blaauw A., Elvius T., 1965, *Stars and Stellar Systems Vol. 5*, “Galactic Structure”, A. Blaauw and M. Schmidt eds., 589
- Carraro G. Chiosi C., 1994, *A&A* 287, 761
- Chaboyer B., Demarque P., Sarajedini A., 1996, *ApJ* 459, 558
- Chen B., 1996, *A&A* 306, 733
- Chiu L.T.G., 1980, *ApJS* 44, 31
- Cohen M., 1995, *ApJ* 444, 874
- Conti P.S., Vacca W.D., 1990, *AJ* 100, 431
- Edvardsson B., Andersen J., Gustaffson B., et al., 1993, *A&A* 275, 101
- Faber S.M., Burstein D., Tinsley B., King I.R., 1976, *AJ* 81, 45
- Fenkart R., Esin-Yilmaz F., 1983, *A&AS* 54, 423
- Freeman K.C., 1992, *IAU Symposium 149*, in ‘The stellar populations of galaxies’, B. Barbuy and A. Renzini (eds.), 65
- Friel E.D., Cudworth K.M., 1986, *AJ* 91, 293
- Gilmore G., Reid N., Hewett P., 1985, *MNRAS* 213, 257 (GRH85)
- Girardi L., Bressan A., Chiosi C., 1996a, *Proceedings ‘Stellar evolution: what should be done’*, 3–5 July 1995, Liège (Belgium), A. Noels et al. (eds.), 39
- Girardi L., Bressan A., Chiosi C., Bertelli G., Nasi E., 1996b, *A&AS* 117, 113
- Hammersley P.L., Garzón F., Mahoney T., Calbet X., 1995, *MNRAS* 273, 206
- Hartwick F.D.A., 1987, in ‘The Galaxy’, G. Gilmore and B. Carswell (eds.), Dordrecht: Reidel, 281
- Huebner W.F., Merts A.L., Magee N.H., Argo M.F., 1977, *Los Alamos Scientific Laboratory Report LA-6760-M*
- Humphreys R.M., Larsen J.A., 1995, *AJ* 110, 2183
- Iglesias C.A., Rodgers F.J., Wilson B.G., 1992, *ApJ* 397, 717
- Jønch-Sørensen H., Knude J., 1994, *A&A* 288, 139
- Kaufer A. Szeifert Th., Krenzlin R., Baschek B., Wolf B., 1994, *A&A* 289, 740
- Kent S.M., Dame T., Fazio G., 1991, *ApJ* 378, 131
- Kinman T.D., Suntzeff N.B., Kraft R.P., 1994, *AJ* 108, 1723
- Koo D.C., Kron R.G., 1982, *A&A* 105, 107
- Kron R.G., 1980, *ApJS* 43, 305
- Kroupa P., Tout C., Gilmore G., 1993, *MNRAS* 262, 545
- Maciel W., Koppen J., 1994, *A&A* 282, 436
- Majewski S.R., 1992, *ApJS* 78, 87
- Majewski S.R., 1993, *ARA&A* 31, 575
- Mera D., Chabrier G., Baraffe I., 1996, *ApJ* 459, L87
- Minniti D., 1995, *AJ* 109, 166
- Mihos J.C., Hernquist L., 1996, *ApJ* 464, 641
- Morrison H.L., Flynn C., Freeman K.C., 1990, *AJ* 100, 1191
- Mould J., 1996, *PASP* 108, 35
- Murray C.A., Argyle R.W., Corben P.M., 1986, *MNRAS* 223, 629
- Ng Y.K., 1994, Ph.D. thesis, Leiden University, the Netherlands
- Ng Y.K., 1996, *Proceedings ‘The impact of large-scale near-IR sky surveys’*, 24–26 April 1996, Puerto de la Cruz (Tenerife; Spain), P. Garzon-Lopez (ed.), *in press*
- Ng Y.K., Bertelli G., Bressan A., Chiosi C., Lub J., 1995, *A&A* 295, 655 (Paper I; erratum *A&A* 301, 318)
- Ng Y.K., Bertelli G., Chiosi C., Bressan A., 1996a, *A&A* 310, 771 (Paper III)
- Ng Y.K., Bertelli G., Chiosi C., Bressan A., 1996b, ‘Spiral Galaxies in the near IR’, *Garching bei München*, 7–9 June 1995, D. Minniti and H.-W. Rix (eds.), 110
- Norris J.E., 1994, *ApJ* 431, 645
- Ojha D.K., Bienaymé O., Robin A.C., Mohan V., 1994, *A&A* 284, 810 (OBRM94)
- Ojha D.K., Bienaymé O., Robin A.C., Crézé M., Mohan V., 1996, *A&A* 311, 456
- Paczyński B., Stanek K.Z., Udalski A., et al., 1994, *AJ* 107, 2060
- Phelps R.L., Janes K.A., Montgomery K.A., 1994, *AJ* 107, 1079
- Piatti A.E., Claria J.J., Abadi M.G., 1995, *AJ* 110, 2813
- Prantzos N., Aubert O., 1995, *A&A* 302, 69
- Rodgers F.J., Iglesias C.A., 1992, *ApJS* 79, 507
- Quinn P.J., Hernquist L., Fullager D.P., 1993, *ApJ* 403, 74
- Reid N., 1990, *MNRAS* 247, 70 (RD90)
- Reid N., Majewski S.R., 1993, *ApJ* 409, 635 (RM93)
- Richtler T., 1994, *A&A* 287, 517
- Robin A., Crézé M., 1986, *A&AS* 64, 53
- Robin A.C., Crézé M., Mohan V., 1992, *A&A* 253, 389
- Robin A.C., Haywood M., Crézé M., Ojha D.K., Bienaymé O., 1996, *A&A* 305, 125
- Ryan S.G., Lambert D.L., 1995, *AJ* 109, 2068
- Spagna A., Lattanzi M.G., Lasker B.M., et al., 1996, *A&A* 311, 758
- Stobie R.S., Ishida K., 1987, *AJ* 93, 624 (SI87)
- Soubiran C., 1992, *A&A* 259, 394
- Steinmetz M., Müller E., 1995, *MNRAS* 276, 549
- Tinney C.G., 1995, *ApJ* 445, 1017
- van Tulder, J.J.M., 1942, *Bull. Astron. Inst. Netherlands* 9, 315
- Unavane M., Wyse R.F.G., Gilmore G., 1996, *MNRAS* 278, 727
- Vandenberg D.A., 1985, *ApJS* 58, 711
- Walker I.R., Mihos J.C., Hernquist L., 1996, *ApJ* 460, 121
- Weistrop D., 1972, *AJ* 77, 366
- Wesselink Th.J.H., 1987, Ph.D. thesis, Catholic University of Nijmegen, the Netherlands
- Yamagata T., Yoshii Y., 1992, *AJ* 103, 117 (YY92)
- Yoshii Y., Ishida K., Stobie R.S., 1987, *AJ* 93, 323
- Zinn R., 1985, *ApJ* 293, 424

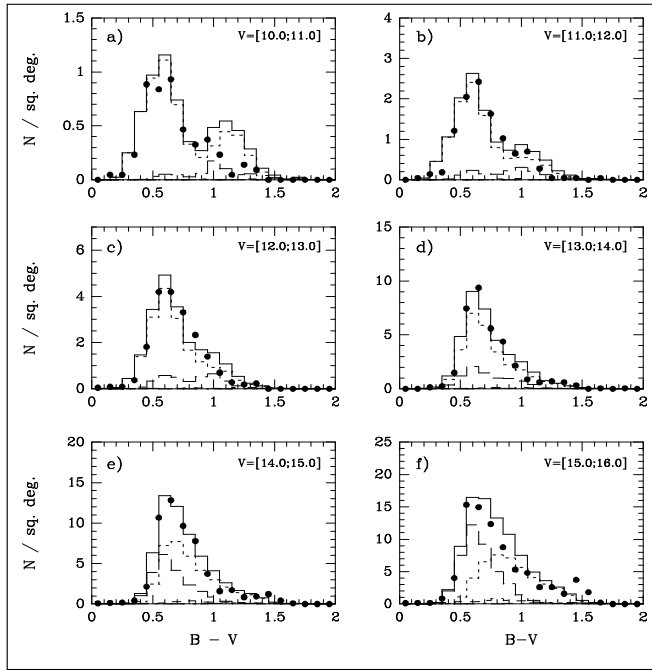


**Fig. 1.1.** Colour distribution from Stobie & Ishida (1987: filled dots) in the direction of the NGP, see text for additional details; solid line for the combined contribution from all populations, dotted line for the young + intermediate disc, long dashed line for the old + thick disc, dashed line for the halo, and dot - long dashed line for the bulge

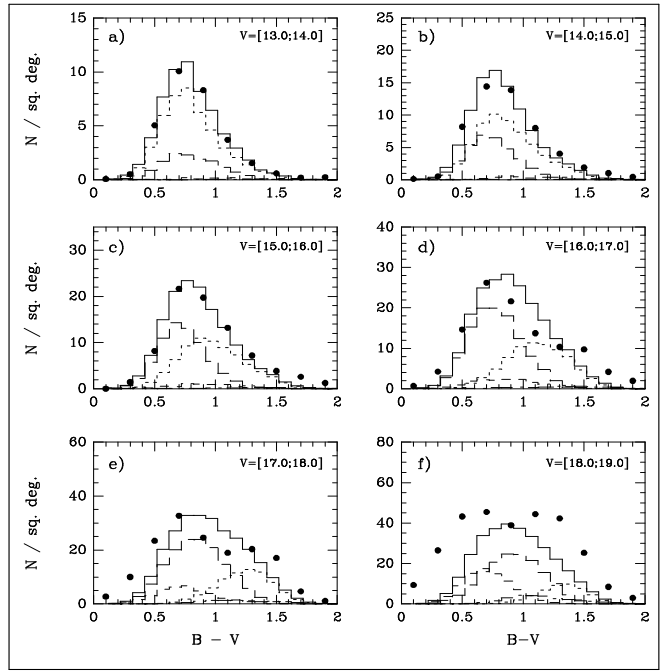


**Fig. 1.2.** Colour distribution from Reid (1990: filled dots) in the direction of the NGP; see text and Fig. 1.1 for additional details

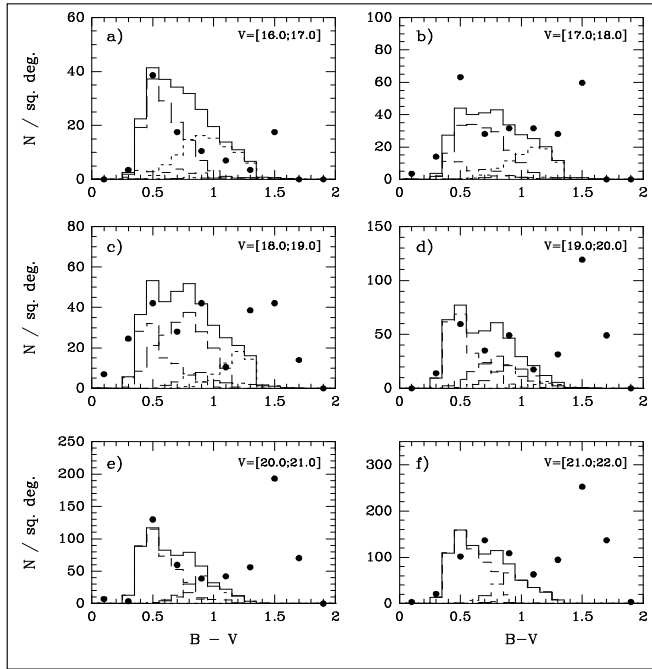


**Fig. 1.3.** Colour distribution from Reid & Majewski (1993: filled dots) in the direction of the NGP; see text and Fig. 1.1 for additional details

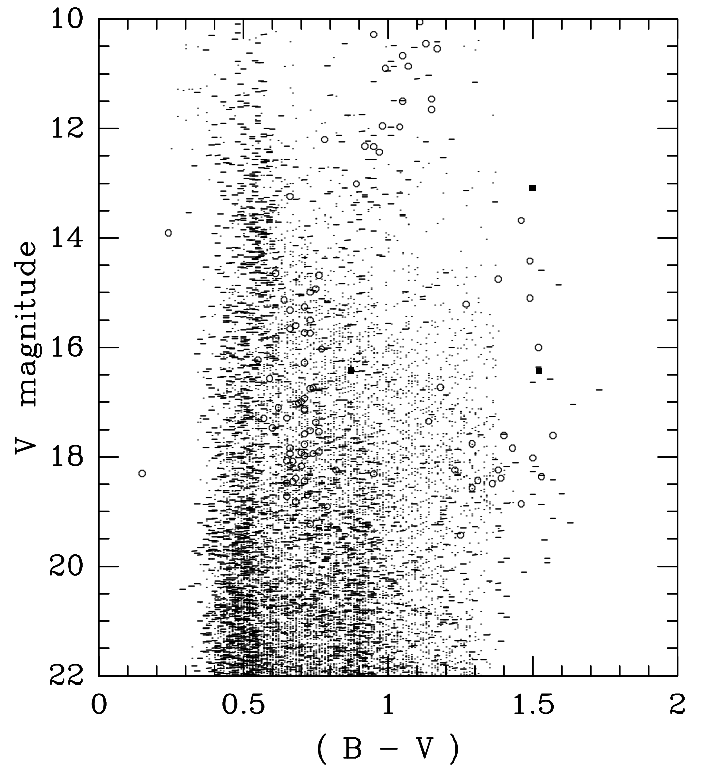


**Fig. 2.0.** Simulated  $(V,B-V)$  CMD ( $5.0 \text{ degree}^2$ ) from the combined stellar populations in the direction of the NGP, see text for other details. Small dots — MS stars, dashes — core H-exhausted or RGB stars, open dots — HB stars, and filled squares for AGB stars

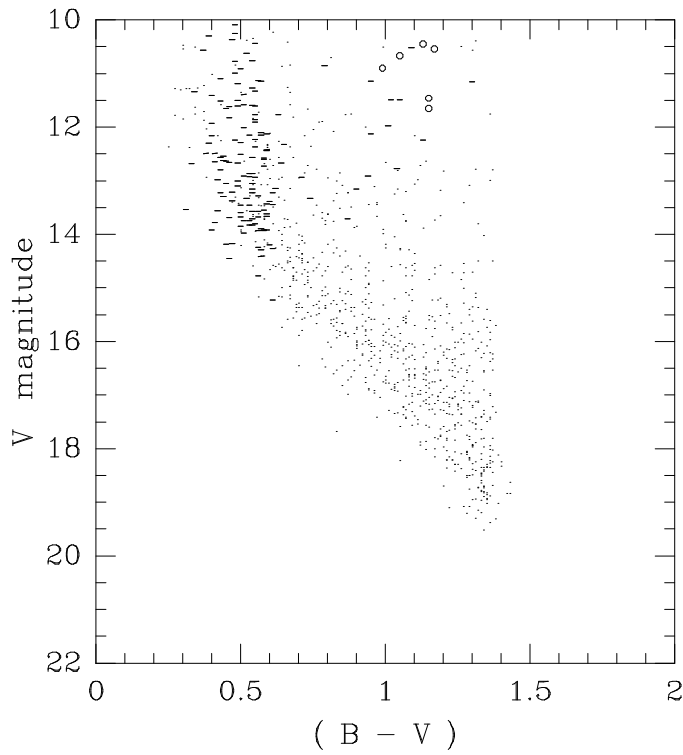


**Fig. 2.1.** Simulated (V,B-V) CMD for the young disc population in the direction of the NGP, see Fig. 2.0 for the symbols and Table 1 for details

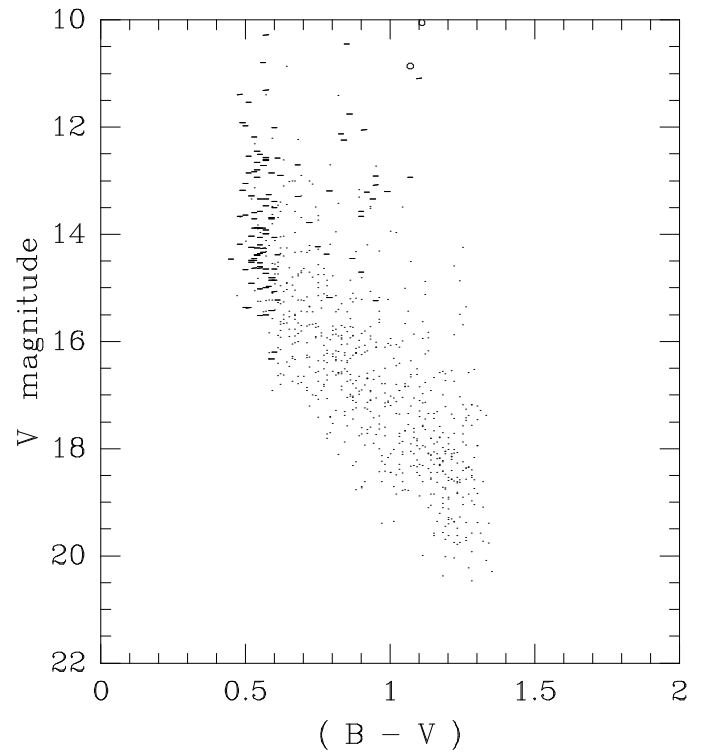


**Fig. 2.2.** Simulated (V,B-V) CMD for the intermediate aged disc population in the direction of the NGP, see Fig. 2.0 for the symbols and Table 1 for details

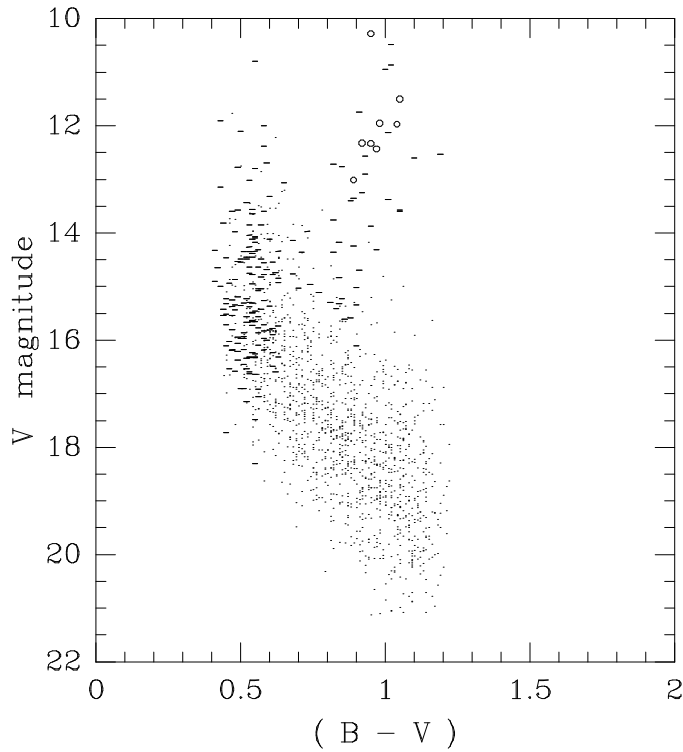


**Fig. 2.3.** Simulated (V,B-V) CMD for the old disc population in the direction of the NGP, see Fig. 2.0 for the symbols and Table 1 for details

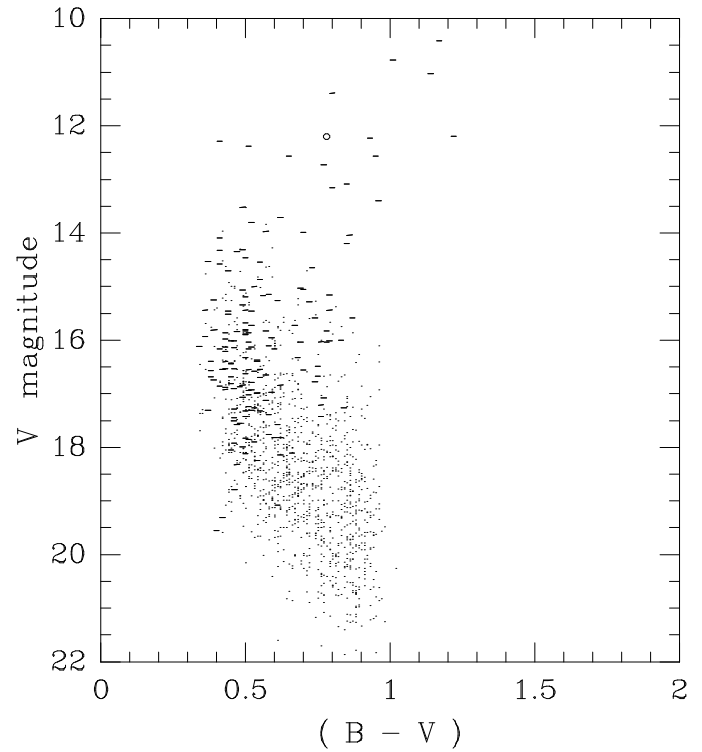


**Fig. 2.4.** Simulated (V,B-V) CMD for the thick disc population in the direction of the NGP, see Fig. 2.0 for the symbols and Table 1 for details

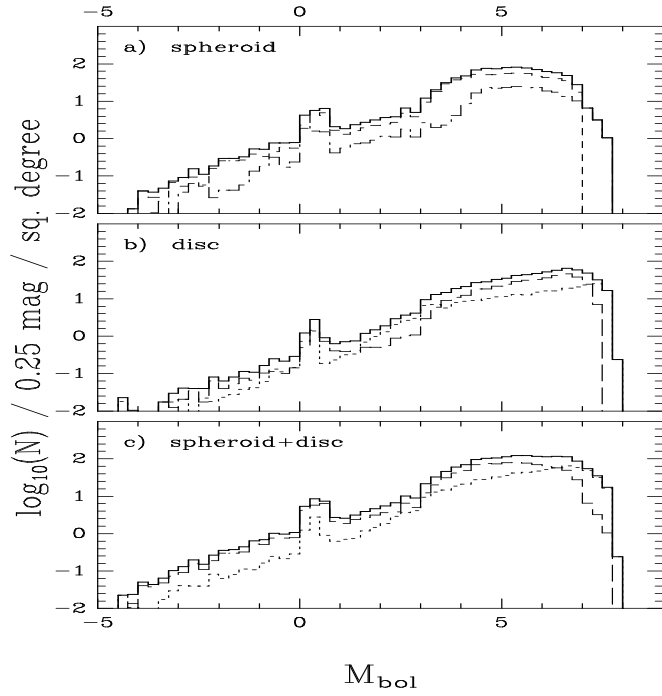


**Fig. 3.1.** Luminosity function for the stars in the MC simulations shown in Figs. 1.1, 1.2, and 1.3 in a) the spheroid, b) the disc, and c) spheroid+disc. See Fig. 1.1 for the line types of the histograms from the frames a and b. In frame c the long dashed histogram is for the spheroid and the dotted histogram for the disc contribution

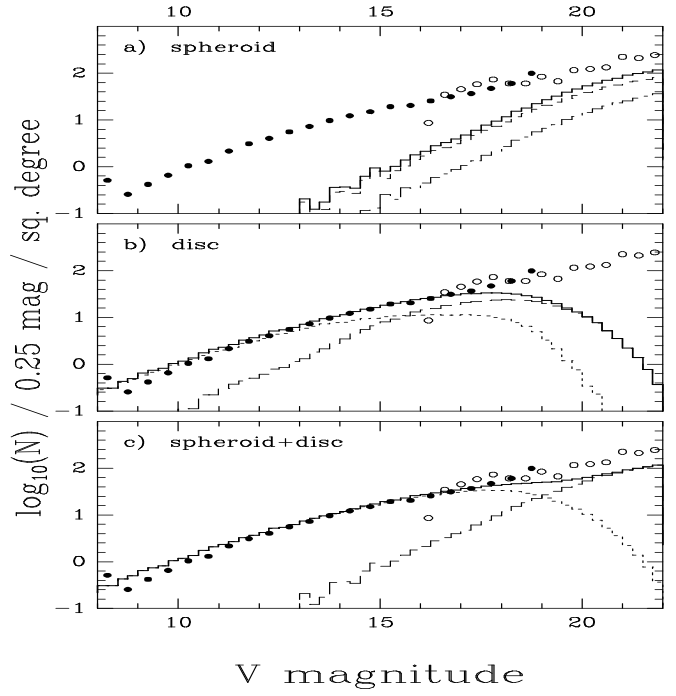


**Fig. 3.2.** Star counts for the colour distributions from the MC simulations shown in Figs. 1.1, 1.2, and 1.3. Filled dots for star count data from SI87 and open dots for data from RM93, see captions of Figs. 1.1 and 3.1 for additional details

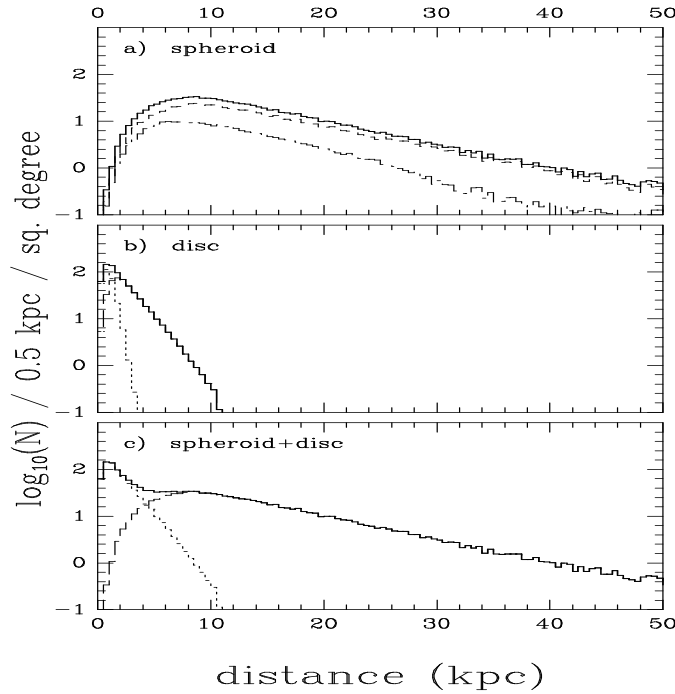


**Fig. 3.3.** Distance distribution for the stars in the MC simulations shown in Figs. 1.1, 1.2, and 1.3. See captions of Figs. 1.1 and 3.1 for additional details

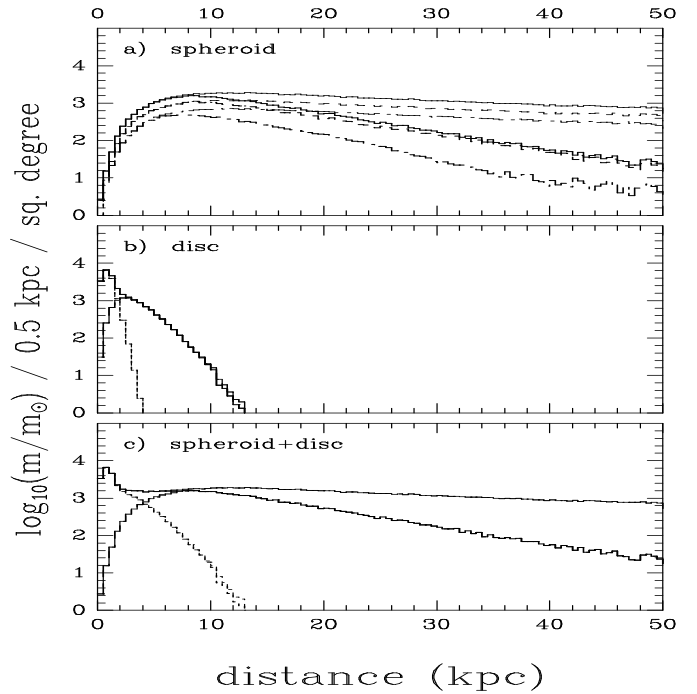


**Fig. 3.4.** Mass density along the line of sight from the MC simulations shown in Figs. 1.1, 1.2, and 1.3. The thick lines denote the ‘visible’ mass and the thin lines the ‘total’ mass present in the line of sight, see captions of Figs. 1.1 and 3.1 for additional details

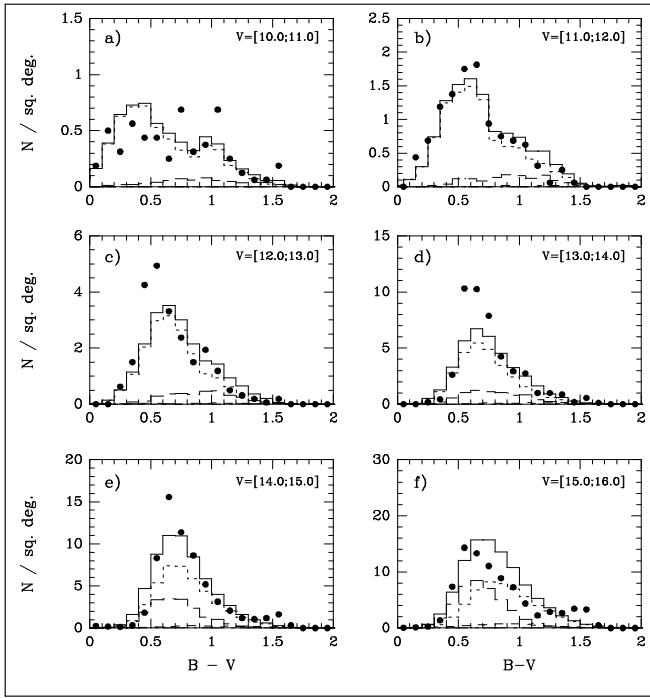


**Fig. 5.1.** Colour distribution from Yamagata & Yoshii, (1992, filled dots) in the direction of the Galactic Anti-Centre; see text and Fig. 1.1 for additional details

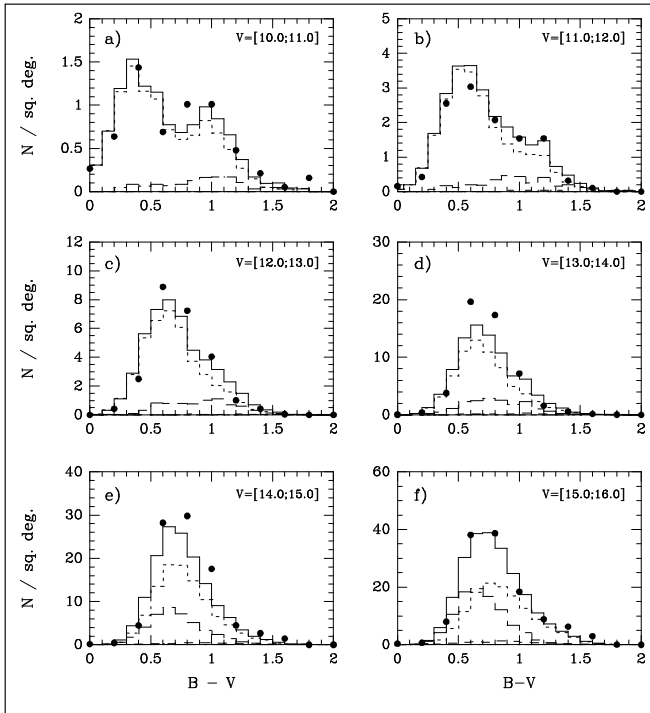


**Fig. 6.1.** Colour distribution from Ojha et al. (1994, filled dots) in the direction of the Galactic Anti-Centre; see text and Fig. 1.1 for additional details

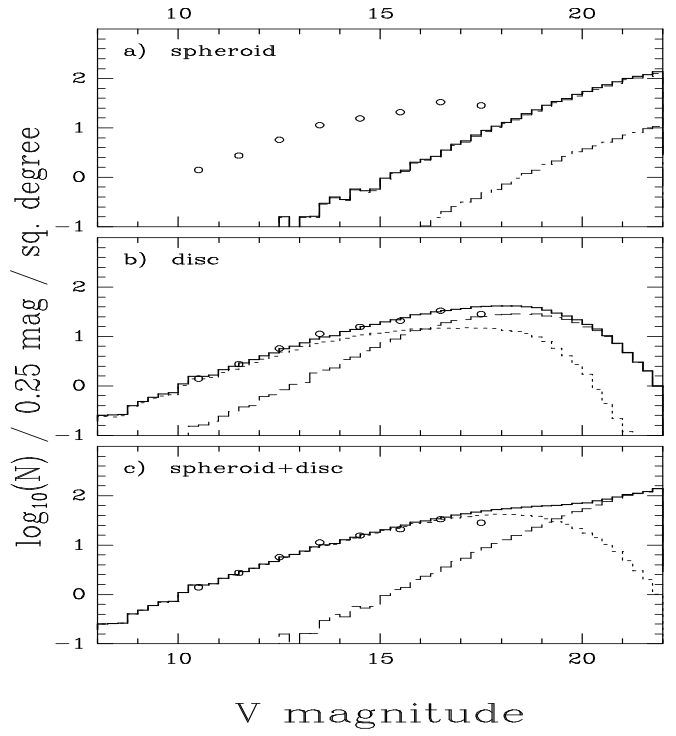


**Fig. 5.2.** Star counts from the MC simulations shown in Fig. 5.1. Open dots are the star counts from YY92, see captions of Figs. 1.1 and 3.1 for additional details

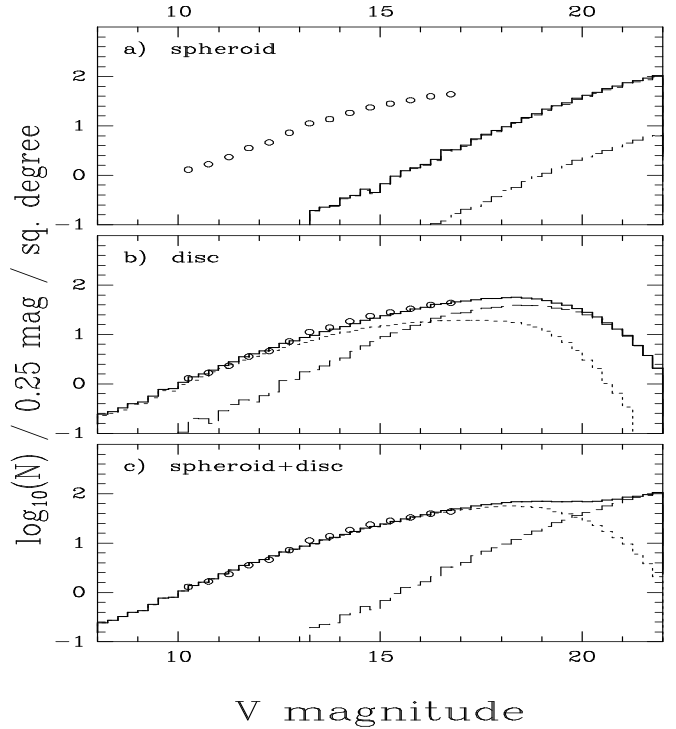


**Fig. 6.2.** Star counts from the MC simulations shown in Fig. 6.1. Open dots are the star counts from Ojha et al. (1994), see captions of Figs. 1.1 and 3.1 for additional details